

# Production of Sustainable Low-Layer Graphene by Green Synthesis at Room Conditions for Platinum-Based Direct Methanol Fuel Cell

Published as part of the ACS Engineering Au virtual special issue "Sustainable Energy and Decarbonization VSI".

Vildan Erduran, Ramazan Bayat, Iskender Isik, Tugba Bayazit, and Fatih Şen\*



Cite This: *ACS Eng. Au* 2023, 3, 537–545



Read Online

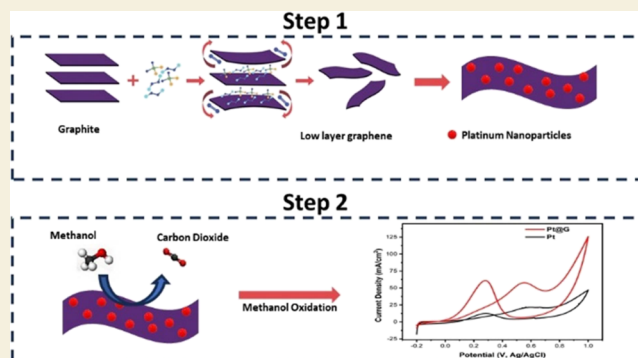
ACCESS |

Metrics & More

Article Recommendations

**ABSTRACT:** In this study, a cost-effective and scalable method for the production of low-layer graphene (LLG) using sodium percarbonate (SPC) as a green delamination agent and its application in fuel cells is proposed. The obtained graphene showed a decrease in signal height in XRD analysis, indicating thinner layers. Raman analysis confirmed the presence of 7–8 layers of graphene. Field-emission scanning electron microscopy analysis revealed a uniform crystal structure, making it suitable for various applications. Direct methanol fuel cells (DMFCs) are widely recognized as efficient and environmentally friendly devices for converting chemical energy to electrical energy. The utilization of graphene-supported platinum (Pt) nanoparticles (NPs) as catalysts in DMFCs enhances their performance. In this study, Pt-graphene catalysts were synthesized by the chemical reduction method with graphene obtained by using SPC. Characterization through XRD and SEM analyses confirmed the homogeneous distribution of NPs on the carbon support. As a result of methanol oxidation studies, 57.73 and 21.45 mA/cm<sup>2</sup> values were obtained by using Pt@LLG and Pt catalysts, respectively. As a result of long-term stability and durability tests, it has been found that the Pt@LLG catalyst can be used effectively in metal oxidation experiments.

**KEYWORDS:** low layer graphene, carbon, green synthesis, direct alcohol fuel cells, electrocatalysts, platinum



## 1. INTRODUCTION

Graphene is a 2D material that consists of a single-atom-thick layer of carbon and has unique electrical, mechanical, and thermal properties. While the carbon atoms that make up the graphene are sp<sup>2</sup> hybridized, they have the extraordinary abilities mentioned thanks to the vacant pz orbitals. Graphene, which is 200 times stronger than steel of the same size, has excellent conductivity, is transparent, and bendable at the same time, has made it the focus of attention of researchers and scientists in recent years due to these excellent properties. Graphene is a promising material for many industrial applications. However, graphene production is often costly and complex.<sup>1–3</sup> The synthesis of graphene can be achieved through various methods, such as the mechanical peeling (exfoliation) method, chemical vapor deposition method, chemical reduction method, arc discharge method, and others, from both bottom-up and top-down approaches. However, many synthesis methods require high temperatures, high pressures, and the use of toxic gases. Hence, the search for a low-cost, easy, and environmentally friendly graphene synthesis method continues.<sup>4–8</sup> The production of graphene, which has

been increasingly used in applications in science and technology in recent years, is important in terms of its high dimensions and quality. Because, in most of the methods mentioned, graphene can be produced in laboratory dimensions, while industrial applications require high-dimensional production. In addition, the removal of the chemicals used in the chemical reduction method and the purification of graphene are very time-consuming and difficult. In addition, the application of these methods requires high temperatures and long processes.<sup>9</sup> In recent years, toxic substances such as sulfuric acid have been used for the chemical peeling method, which has been widely used in the production of high-capacity graphene. The use of these substances poses a danger to human health and the environment both during the

**Received:** August 9, 2023

**Revised:** October 10, 2023

**Accepted:** October 11, 2023

**Published:** November 29, 2023

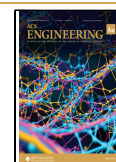




**Figure 1.** Graphene was obtained from graphite at room temperature.

application, during the purification phase, and during the postprocessing waste generation.<sup>8–10</sup> Green synthesis of low-layer graphene (LLG) at room temperature has emerged as a cheaper and simpler production method. This method is accomplished by adding a reducing agent to graphene oxide in a solution. Reducing agents used in this method include chemicals such as hydrazine, sodium borohydride, ascorbic acid, and SPC.<sup>11,12</sup> The type and concentration of the reducing agent can affect graphene quality and properties. Therefore, graphene manufacturers should be aware that various parameters need to be examined in order to optimize the synthesis parameters.<sup>13–15</sup> Developments in graphene production methods also enable developments in the field of energy. In order to address the pressing environmental concerns and meet the growing energy demands of humanity, it is necessary to explore alternative energy sources that can replace the current reliance on fossil fuels like petroleum and natural gas.<sup>16,17</sup> Among these alternatives, direct methanol fuel cells (DMFCs) offer a promising solution by directly converting chemical energy into electrical energy.<sup>18,19</sup> They have gained considerable attention as environmentally friendly power sources for portable electronics and vehicles.<sup>20</sup> In DMFCs, methanol reacts with oxygen from the air, resulting in the production of carbon dioxide and water, which generates electricity.<sup>21,22</sup> The electrocatalysts used in DMFCs, specifically platinum-based (Pt-based) catalysts, play a crucial role in facilitating the methanol oxidation and oxygen reduction reactions at the anode and cathode, respectively. However, the limited practical application of Pt catalysts in DMFCs is mainly attributed to their low utilization efficiency and high cost per unit area. Advances in nanotechnology have accelerated progress in many fields.<sup>23–25</sup> To overcome this challenge, researchers have explored different types of carbon supports including single-walled carbon nanotubes, multiwalled carbon nanotubes, cup-stacked-type carbon nanotubes, and graphitic carbon nanofibers. These carbon supports exhibit excellent conductivity and serve as effective platforms for uniformly dispersing platinum nanoparticles (Pt NPs).<sup>22,26–29</sup>

Graphene, with its intriguing two-dimensional structure, has emerged as a promising carbon support material for Pt NPs, offering several notable advantages.<sup>30,31</sup> Its exceptional conductivity ( $10^3$ – $10^4$  S/m), substantial theoretical surface area (calculated value,  $2600\text{ m}^2/\text{g}$ ), unique graphitized basal plane structure, and potential for cost-effective manufacturing have made it the subject of extensive research in recent years.<sup>32</sup> Various techniques, such as chemical reduction and electrochemical reduction, have been successfully employed to synthesize graphene-supported Pt NPs nanocomposites with distinct structural features, including nanospheres, nanofibers, nanowires, nanotubes, nanosheets, nanowheels, nanocages, and nanodendrites. Despite the progress made in depositing Pt NPs onto graphene nanolayers, achieving precise control over

dimensions and morphologies, as well as achieving effective Pt NP loading, still presents significant challenges.<sup>33–35</sup>

The use of carbon-based nanomaterials with outstanding characteristics such as low cost and high surface area is also noteworthy for reducing the cost and ensuring high performance of Pt-based fuel cells.<sup>36</sup> Among carbon-based nanomaterials, graphene stands out as a potential candidate for alcohol electrooxidation due to its unique electrical and structural properties, excellent flexibility, and high surface area.<sup>37,38</sup>

In this study, a new method is proposed in which chemicals such as sulfuric acid are used very little, and SPC is used instead, in order to decompose the graphite into flaky layers. Thanks to SPC, active oxygen, and soda it provides to the aquatic environment. It has strong bleaching, sterilizing, water-softening, cleaning, and deodorizing properties. In addition, it is an environmentally friendly chemical, as it is odorless and does not contain any chemicals harmful to human health and the environment. Green synthesis of LLG under room conditions with this method is a promising method for graphene production. Green chemistry represents an area called environmentally friendly chemistry, and synthesis methods are also considered in this context. For this purpose, LLG synthesis, which can be performed at room conditions, stands out among the green synthesis methods. This method is cheaper, environmentally friendly, scalable, and potentially useful for industrial applications.<sup>39</sup> In this study, we also report an easy, efficient, and controllable approach of utilizing the structure obtained by dispersing Pt NPs onto the produced few-layered graphene for direct methanol-alcohol fuel cell applications. The prepared Pt/graphene nanocomposites were characterized by using scanning electron microscopy (SEM), energy-dispersive spectroscopy, X-ray diffraction (XRD) spectroscopy, and Raman spectroscopy. The electrocatalytic activity of Pt/graphene was investigated by using methanol oxidation and oxygen reduction as model systems. The results demonstrated significant electrocatalytic activities of Pt/graphene nanocatalysts with high electrochemically active surface area toward both electrode reactions. The present study offers an interesting strategy for preparing graphene-based catalysts using SPC for DMFC applications.

## 2. MATERIAL AND METHOD

### 2.1. Materials

Graphite (C), concentrated  $\text{H}_2\text{SO}_4$  (95–98%), and sodium percarbonate (SPC) were supplied from Sigma-Aldrich, Isolab, Akbel chemical company, respectively. Methanol (99.9%), platinum(II) chloride ( $\text{PtCl}_2$ , 99.9%), sodium borohydride ( $\text{NaBH}_4$ , 98%) sulfuric acid ( $\text{H}_2\text{SO}_4$ , 97%), and dimethylformamide (DMF, 99%) have been purchased from Sigma-Aldrich, and Nafion D-521 solution (5%) has been purchased from Alfa Aesar.

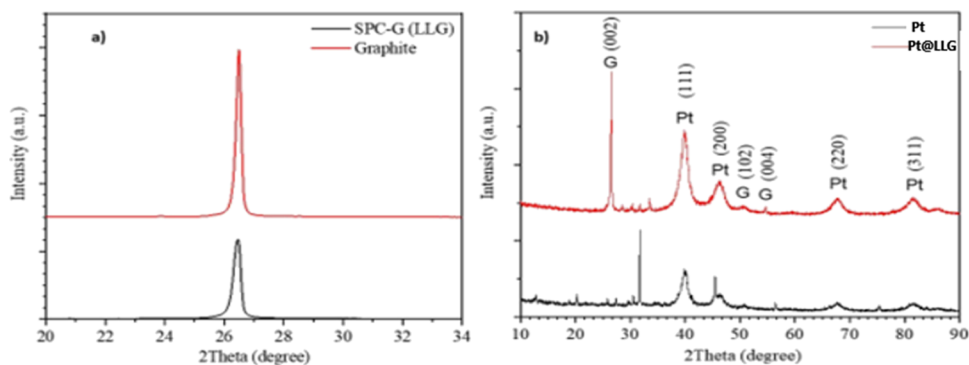


**Figure 2.** X-ray diffraction (XRD) patterns of graphite and low-layer graphene synthesized with (a) sodium percarbonate (SPC-G) and (b) Pt and Pt@LLG powders.

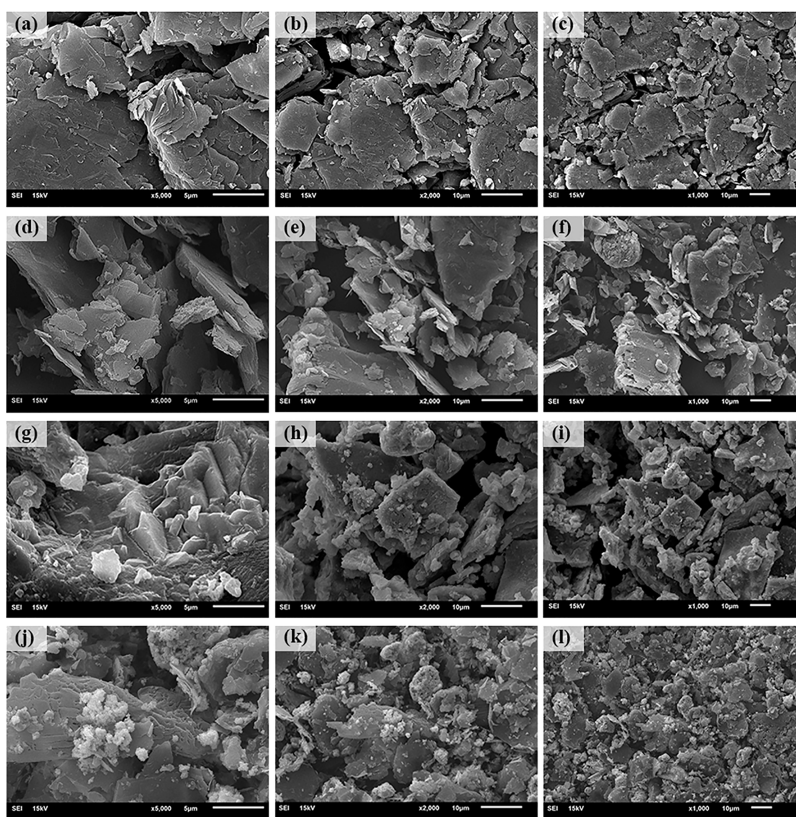


**Figure 3.** Field-emission scanning electron microscopy (FESEM) images of low-layer graphene (LLG) (a–l).

## 2.2. Synthesis of LLG

1 g of graphite and 4 g of SPC were combined in a beaker using a basic stirring rod for 10 s to achieve a uniform distribution of the particles. Following this, 10 mL of  $\text{H}_2\text{SO}_4$  solution was added to the mixture, and further mixing was conducted using the same stirring rod. The mixture was not subjected to sonication. Subsequently, the mixture was allowed to sit at room temperature for a duration of 3 h. Upon completion of the 3 h period, the mixture was rinsed with distilled water until reaching a pH of 7. The resulting material was air-dried at room temperature (Figure 1).<sup>40</sup>

## 2.3. Synthesis of Electrocatalysts

Electrocatalysts to be used in methanol oxidation studies were prepared using LLG-supported platinum (Pt@LLG) and platinum (Pt) using the chemical reduction method. 10 mM  $\text{PtCl}_2$  and 50 mg of LLG were mixed in 20 mL of  $\text{dH}_2\text{O}$ . Then,

this solution was mixed on a magnetic stirrer for 30 min and subjected to sonication. 80 mg of  $\text{NaBH}_4$  was added to the medium and mixed in a magnetic stirrer until the hydrogen gas evolution ceased. After the reduction process was completed, the Pt@LLG electrocatalyst formed was collected by centrifugation at 4000 rpm and dried at room temperature. The same process was repeated to use the Pt catalyst without using LLG.<sup>41,42</sup>

## 2.4. Electrochemical Measurements

An electrode solution was prepared for the synthesized Pt-graphene catalysts. Electrode solutions were prepared by mixing 10 mg of Pt-graphene, 75  $\mu\text{L}$  of Nafion, 150  $\mu\text{L}$  of DMF, and 500  $\mu\text{L}$  of distilled water, and then, 15  $\mu\text{L}$  of the resulting mixture was dropped onto a 3 mm diameter glassy carbon electrode surface and allowed to dry. The three-electrode cell system was connected to a potentiostat/

galvanostat (Gamry Interface 1000, USA) device for the measurements. In the three-electrode system, a glassy carbon electrode, platinum plate, and Ag/AgCl electrode were used as the working electrode, counter electrode, and reference electrode, respectively, and the system was purged with nitrogen gas for 2 min prior to the measurements to remove oxygen from the electrochemical cell. To evaluate the electrocatalytic performance of Pt/graphene nanocomposites, their methanol oxidation ability in 1.0 M H<sub>2</sub>SO<sub>4</sub> solution containing 1 M CH<sub>3</sub>OH was investigated. The oxidation reactions were studied by using a scan rate of 50 mV/s. These measurements were conducted to determine the nanocomposites' overall electrocatalytic capabilities.<sup>33</sup>

### 3. RESULTS AND DISCUSSION

This study offers a low-cost, green, and easily scalable graphene production method; further characterization of graphene was performed by several techniques, such as XRD (Rigaku Smartlab, Japan), field-emission scanning electron microscopy (FESEM, JEOL JSM 6610, Japan), and Raman spectroscopy.

Overall, XRD analysis is shown in Figure 2a as an important tool for determining the structural properties of graphene samples. The result of XRD analysis for graphene is often used to distinguish between bilayer graphene and monolayer graphene. Double-layer graphene generally has a finer peak structure because the distance between the two graphene layers is shorter.<sup>43,44</sup> The XRD patterns of Pt and Pt-G powders are shown in Figure 2b. As can be seen in Figure 2b, the XRD pattern of Pt powder is dominated by peaks located at 39.80° (111) and 46.28° (200). All of these peaks are found to be compatible with the JCPDS 01-087-0646 card of the cubic Pt structure.<sup>45</sup> In addition, apart from these peaks, there are low-intensity peaks. In addition, when the XRD of the Pt-G powder was examined in detail, both graphite and platinum peaks were found. Upon examination of the XRD pattern of the powder, the presence of peaks corresponding to the cubic Pt structure was observed, in addition to the peaks associated with the hexagonal C structure, as indicated by JCPDS 01-087-0646 and JCPDS 03-065-6212 cards, respectively.

As a result of FESEM analysis of graphite and graphene in comparison to FESEM images shown in Figure 3a–l, high resolution images are obtained for the samples. These images are used to observe surface properties, such as thickness, smoothness, roughness, cracks, and defects of graphene samples. In addition, SEM images can also determine the size and shape of graphene samples. FESEM images can be used to study the properties of graphene flakes. Density profiles can be obtained from SEM images made at different acceleration voltages. As the thickness increases, the density of the secondary electrons decreases. At high accelerating voltages, more secondary electrons are emitted from the substrate than the graphene flakes, resulting in a small density change. At low accelerating voltages, fewer secondary electrons are emitted from the substrate than the graphene flakes, and the density ratio increases. Graphene can be seen more clearly at low acceleration voltages because incoming electrons pass through graphene quickly. The variation in contrast based on graphene thickness can be explained by differences in secondary electron emission.<sup>46,47</sup>

The resulting FESEM images are typical FESEM images of a graphene flake. The actual intensity profiles shown in Figure 3 were obtained from FESEM images of the same region at various acceleration voltages. At certain points where thickness

variations occur, the density of the detected secondary electrons decreased as the thickness increased.<sup>48,49</sup>

In graphene samples, the Raman spectrum provides information about the structural properties of the sample, such as thickness, purity, defect density, crystal structure, and orientation. The ratio between the 2D and G bands corresponds to the thickness of the graphene. In addition, the intensity of the D band corresponds to the defect density of the sample. As a result of Raman analysis, 2D, G and D bands of graphene are observed. The G band originates from the C–C bonds in the crystal structure of graphene and is usually seen at 1580 cm<sup>-1</sup>. The 2D band corresponds to the characteristic vibrational mode in the 2D structure and is usually seen around 2700 cm<sup>-1</sup>. The D band originates from defects in graphene and is usually seen around 1350 cm<sup>-1</sup>.<sup>49–52</sup>

In Raman spectroscopy, the D band is seen as the first peak in the range 1000–2000 cm<sup>-1</sup>, while the G band is seen as the second peak. The 2D band is determined by the peak in the range 2000–3000 cm<sup>-1</sup>. The G band is observed in all carbon-based materials that undergo sp<sup>2</sup> hybridization, while the 2D band is unique to graphene and plays an important role in the characterization of graphene. The D/G ratio is used to determine the purity of the graphene, and the lower this ratio, the better the purity of the graphene. The position and shape of the 2D band are used to determine the number of graphene layers. As seen in Figure 4, the 2D band of the graphene is

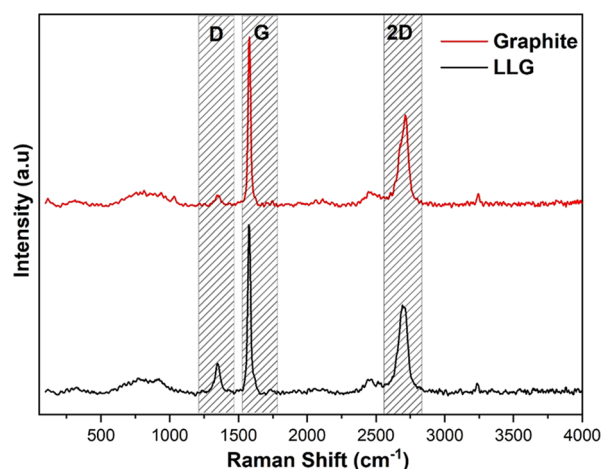


Figure 4. Raman analysis of several-layer graphene obtained under room conditions.

observed at 2700 cm<sup>-1</sup>, while it is observed at 2695 points of LLG. The shift of the 2D band to the left is one of the expressions indicating that the number of layers is decreasing.<sup>53</sup> In addition, the two points of the 2D band around 2700 cm<sup>-1</sup> are related to the graphene layer thickness. In graphene Raman measurements, the intensity of the D band increases with the number of layers, and the 2D/G band intensity ratio decreases with the number of layers. As shown in Figure 4, the 2D/G ratios of graphite and LLG are 0.53 and 0.52, respectively.<sup>50,53,54</sup>

In the method used in the study, graphene material is produced by an oxidation-low temperature reduction method. SPC is used to destroy the oxygen groups on the graphite surface, and then the bonds between the graphite structures are broken at low temperatures, and graphene material is obtained.<sup>7,40,55</sup>

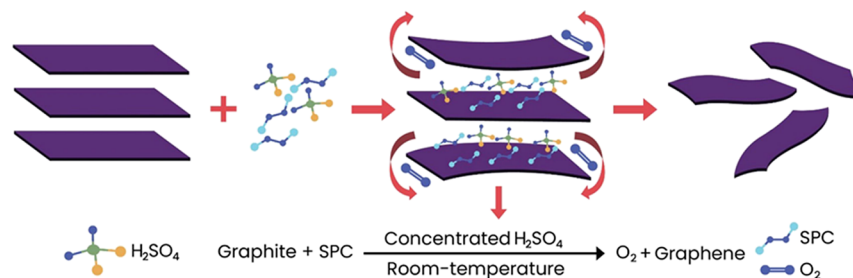


Figure 5. Mechanism of conversion of graphite to graphene by chemical peeling.<sup>40</sup>

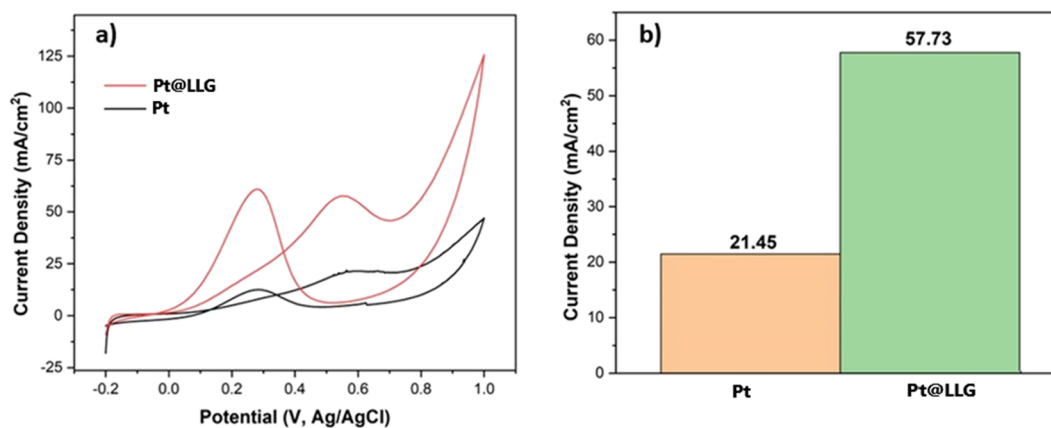


Figure 6. CV curve (a) and bar chart values of Pt and Pt@LLG (b).

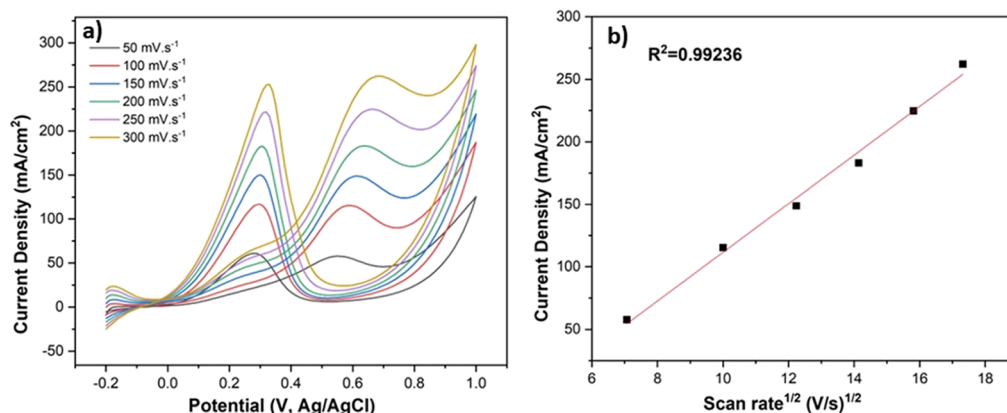


Figure 7. CV of Pt@LLG at different scan rates (a) and square root of scan rate vs peak current density plot (b).

It is an inexpensive and easily applicable method for the production of graphene by the SPC method. This method could be an important step toward increasing the industrial and commercial use of graphene material. The mechanism of conversion of graphite to graphene by chemical peeling is shown in Figure 5.<sup>40</sup> SPC is an environmentally friendly material and less toxic compared to other oxidizing agents. This is an ideal option for researchers looking for environmentally friendly production methods. Graphene obtained using SPC can be produced with a higher yield than other graphene synthesis methods. This allows a higher rate of oxidation of the graphite material and results in more graphene layers.<sup>7,55</sup>

Electrocatalytic methanol oxidation studies of the prepared nanocatalysts were first carried out with CV at 50 mV/s in 1.0 M H<sub>2</sub>SO<sub>4</sub> medium containing 1 M methanol. CV profiles of Pt and Pt@LLG are given in Figure 6a. The onset potentials for

Pt and Pt@LLG were found to be 0.02 V and 0.1, respectively. These results ensured that the use of the graphene support material resulted in a higher anodic peak current density and lower onset potential of Pt@LLG. Examining the curves, going from negative to positive, the Pt and Pt@LLG catalysts show a single peak. The peaks indicate that the methanol is oxidized by the Pt and Pt@LLG catalysts.<sup>56</sup> In Figure 6b, the anodic peak potentials of Pt and Pt@LLG nanocatalysts at 0.55 V potential were determined as 21.45 and 57.73 mA/cm<sup>2</sup>, respectively.

Electrocatalytic reactions occurring on the electrocatalyst surface and transport of reactive substances play an important role in terms of electrocatalytic activity.<sup>57</sup> In this context, CV measurements were carried out at different scanning rates (50–300 mV.s<sup>-1</sup>) in 1.0 M H<sub>2</sub>SO<sub>4</sub> medium containing 1 M methanol using a Pt@LLG electrocatalyst. As seen in Figure 7a, it was observed that the anodic peak current density

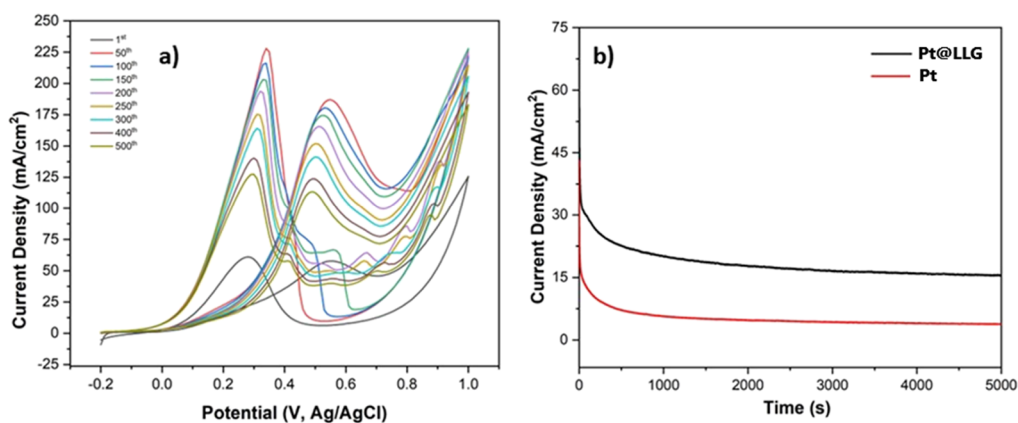


**Figure 8.** Long-term durability test of Pt@LLG (a) and long-term stability measurement of Pt@LLG and Pt (b).

increased depending on the scanning speed. These results indicate that methanol oxidation is subject to a lower kinetic limit as the scanning rate increases.<sup>58</sup> In addition, the current density graph plotted against the square root of the scanning speed in Figure 7b shows that the scanning speed and the current density increase linearly. The results obtained show that methanol works in a diffusion-controlled manner.<sup>57</sup>

The long-term catalytic stability of the catalyst activities is of great importance in electrooxidation studies. In this context, first, 500 CV measurements were taken at a scanning speed of 50 mV/s in 1.0 M H<sub>2</sub>SO<sub>4</sub> medium containing 1 M methanol within the scope of long-term durability study. As seen in Figure 8a, it is seen that the current density increases in the first 50 cycles and then decreases. However, the anodic peak current density obtained after 500 cycles is higher than the initial anodic peak current density. These findings showed that Pt@LLG exhibited long-term durability.

The long-term stability test was performed using CA for 5000 s at 0.55 V in 1.0 M H<sub>2</sub>SO<sub>4</sub> containing 1 M methanol. As seen in Figure 8b, the end current densities for Pt@LLG and Pt catalysts were obtained as 15.64 and 3.82 mA/cm<sup>2</sup>, respectively. It is seen that the initial current densities of Pt@LLG and Pt catalysts decrease rapidly at the beginning and then continue stably as a result of the byproducts and CO coating of the catalyst active sites.<sup>59,60</sup>

In methanol oxidation studies, the ability of the CO to tolerate is of great importance. Therefore, the CO tolerance of Pt@LLG and Pt catalysts was investigated by a CO stripping test. Figure 9 shows the CO stripping plots of Pt@LLG and Pt catalysts. When the CO stripping graphs are examined, it is observed that the CO adsorption of the Pt@LLG catalyst starts at 0.44 V, while that of the Pt catalyst starts at about 0.48 V. The earlier onset of the CO adsorption of the Pt@LLG catalyst indicates that CO oxidation is easier than that of the Pt catalyst. When the peak current points are analyzed, it is seen that the CO adsorption peaks of Pt@LLG and Pt catalysts are 0.6 and 0.55 V, respectively. The results show that the Pt@LLG catalyst shows higher CO poisoning resistance.<sup>61</sup>

Comparison of the results obtained from electrochemical studies is shown in Table 1. Studies conducted with different material types showed that Pt@LLG can be used in DMFC studies.

## Conclusions

This work is focused on the production of multilayer graphene using SPC and its usability as a support material for the Pt

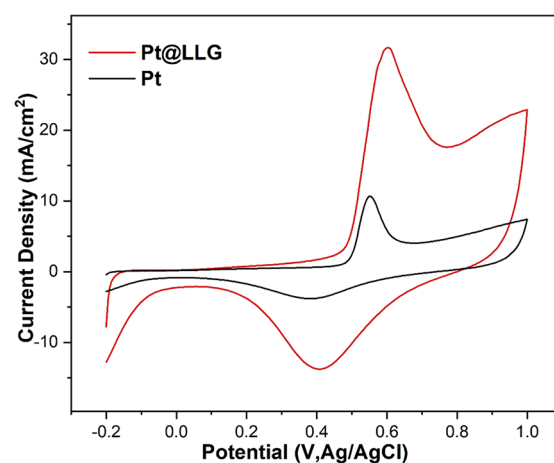


**Figure 9.** Pt@LLG and Pt CO stripping result in 0.5 M H<sub>2</sub>SO<sub>4</sub> at a 25 mV s<sup>-1</sup> scan rate.

**Table 1.** Comparison of the Results Obtained with the Pt@LLG Catalyst with Those of the Literature

electrocatalyst	scan rate (mV s <sup>-1</sup> )	current density (mA cm <sup>-2</sup> )	reference
PtTe PNCs	50	28.94	62
PtCuCo NFs	50	4.24	63
Pt-PVP-01	50	1.38	64
PtRu@CNF	50	48.14	65
Pt@PdS <sub>2</sub> -MWCNT	50	86.71	66
Pt@LLG	50	57.73	this work

catalyst in fuel cells. Several characterization studies carried out showed that the obtained multilayer graphene showed a decrease in signal height in XRD analysis indicating thinner layers, and Raman analysis confirmed the presence of 7–8 graphene layers. According to Raman results, the 2D/G ratios of graphite and LLG are 0.53 and 0.52, respectively. Methanol oxidation studies were carried out to evaluate the performance of Pt@LLG and Pt catalysts in fuel cells. The results showed that the Pt@LLG catalyst achieved a higher electrical current density (57.73 mA/cm<sup>2</sup>), highlighting the potential of Pt-graphene catalysts in improving the efficiency of fuel cells. Furthermore, long-term stability and durability tests and CO stripping studies showed that the Pt@LLG catalyst can be effectively used in methanol oxidation studies. In conclusion, this study demonstrates that LLG obtained using SPC can be successfully used to synthesize efficient catalysts for fuel cells,

and long-term stability and durability are achieved. These results could be an important step toward more environmentally friendly and cost-effective energy production in the future.

## AUTHOR INFORMATION

### Corresponding Author

**Fatih Şen** – Sen Research Group, Department of Biochemistry, Kutahya Dumlupınar University, 43100 Kütahya, Turkey; Kutahya Design & Technopole, SRG Incorporated Company, 43100 Kütahya, Turkey; [orcid.org/0000-0001-9929-9556](https://orcid.org/0000-0001-9929-9556); Email: [fatih.sen@dpu.edu.tr](mailto:fatih.sen@dpu.edu.tr)

### Authors

**Vildan Erduran** – Department of Materials Science & Engineering, Faculty of Engineering, Kutahya Dumlupınar University, 43100 Kütahya, Turkey; Sen Research Group, Department of Biochemistry, Kutahya Dumlupınar University, 43100 Kütahya, Turkey

**Ramazan Bayat** – Department of Materials Science & Engineering, Faculty of Engineering, Kutahya Dumlupınar University, 43100 Kütahya, Turkey; Sen Research Group, Department of Biochemistry, Kutahya Dumlupınar University, 43100 Kütahya, Turkey

**İskender Isik** – Department of Materials Science & Engineering, Faculty of Engineering, Kutahya Dumlupınar University, 43100 Kütahya, Turkey

**Tugba Bayazit** – Central Research Laboratory, Recep Tayyip Erdogan University, 53100 Rize, Turkey

Complete contact information is available at:

<https://pubs.acs.org/10.1021/acseengineeringau.3c00040>

### Notes

The authors declare no competing financial interest.

## REFERENCES

- (1) Nasrollahzadeh, M.; Sajadi, S. M.; Sajjadi, M.; Issaabadi, Z. An Introduction to Nanotechnology. In *Interface Science and Technology*; Elsevier B.V., 2019; Vol. 28, pp 1–27.
- (2) Kai-Hua Chow, E.; Gu, M.; Xu, J. Carbon Nanomaterials: Fundamental Concepts, Biological Interactions, and Clinical Applications. In *Nanoparticles for Biomedical Applications*; Elsevier, 2020; pp 223–242.
- (3) Nehra, M.; Dilbaghi, N.; Hassan, A. A.; Kumar, S. Carbon-Based Nanomaterials for the Development of Sensitive Nanosensor Platforms. In *Advances in Nanosensors for Biological and Environmental Analysis*; Elsevier, 2019; pp 1–25.
- (4) Bhuyan, M. S. A.; Uddin, M. N.; Islam, M. M.; Bipasha, F. A.; Hossain, S. S. Synthesis of Graphene. *Int. Nano Lett.* **2016**, *6* (2), 65–83. 2016 62
- (5) Lee, X. J.; Hiew, B. Y. Z.; Lai, K. C.; Lee, L. Y.; Gan, S.; Thangalazhy-Gopakumar, S.; Rigby, S. Review on Graphene and Its Derivatives: Synthesis Methods and Potential Industrial Implementation. *J. Taiwan Inst. Chem. Eng.* **2019**, *98*, 163–180.
- (6) Wang, X.; You, H.; Liu, F.; Li, M.; Wan, L.; Li, S.; Li, Q.; Xu, Y.; Tian, R.; Yu, Z.; Xiang, D.; Cheng, J. Large-Scale Synthesis of Few-Layered Graphene Using CVD. *Chem. Vap. Deposition* **2009**, *15* (1–3), 53–56.
- (7) Jin, Y.; Huang, S.; Zhang, M.; Jia, M.; Hu, D. A Green and Efficient Method to Produce Graphene for Electrochemical Capacitors from Graphene Oxide Using Sodium Carbonate as a Reducing Agent. *Appl. Surf. Sci.* **2013**, *268*, 541–546.
- (8) Kumar, N.; Kumbhat, S. Carbon-Based Nanomaterials. In *Essentials in Nanoscience and Nanotechnology*; Wiley, 2016; pp 189–236.
- (9) Pirard, S. L.; Douven, S.; Pirard, J. P. Large-Scale Industrial Manufacturing of Carbon Nanotubes in a Continuous Inclined Mobile-Bed Rotating Reactor via the Catalytic Chemical Vapor Deposition Process. *Front. Chem. Sci. Eng.* **2017**, *11* (2), 280–289.
- (10) Ji, M.; Wei, Z.; Ji, M.; Wei, Z. A Review of Water Management in Polymer Electrolyte Membrane Fuel Cells. *Energies* **2009**, *2* (4), 1057–1106.
- (11) Park, S.; An, J.; Potts, J. R.; Velamakanni, A.; Murali, S.; Ruoff, R. S. Hydrazine-Reduction of Graphite- and Graphene Oxide. *Carbon* **2011**, *49* (9), 3019–3023.
- (12) Boro, U.; Karak, N. Tannic Acid Based Hyperbranched Epoxy/Reduced Graphene Oxide Nanocomposites as Surface Coating Materials. *Prog. Org. Coat.* **2017**, *104*, 180–187.
- (13) Ruti, I.; Kumar, S. Bamboo Shoot Extract as a Novel and Efficient Reducing Agent for Graphene Oxide and Its Supercapacitor Application. *J. Mater. Sci. Mater. Electron.* **2023**, *34* (1), 1–14.
- (14) Joshi, R.; De Adhikari, A.; Dey, A.; Lahiri, I. Green Reduction of Graphene Oxide as a Substitute of Acidic Reducing Agents for Supercapacitor Applications. *Mater. Sci. Eng., B* **2023**, *287*, No. 116128.
- (15) Andrijanto, E.; Shoelarta, S.; Subiyanto, G.; Rifki, S. Facile Synthesis of Graphene from Graphite Using Ascorbic Acid as Reducing Agent. In *AIP Conference Proceedings*; AIP Publishing LLC/AIP Publishing, 2016; Vol. 1725, p 020003.
- (16) Hojjati-Najafabadi, A.; Aygun, A.; Tiri, R. N. E.; Gulbagca, F.; Lounissaa, M. I.; Feng, P.; Karimi, F.; Sen, F. Bacillus Thuringiensis Based Ruthenium/Nickel Co-Doped Zinc as a Green Nanocatalyst: Enhanced Photocatalytic Activity, Mechanism, and Efficient H<sub>2</sub> Production from Sodium Borohydride Methanolysis. *Ind. Eng. Chem. Res.* **2023**, *62* (11), 4655–4664.
- (17) Olah, G. A. Beyond Oil and Gas: The Methanol Economy. *Angew. Chem., Int. Ed.* **2005**, *44* (18), 2636–2639.
- (18) Hosseini, V. R.; Mehrizi, A. A.; Karimi-Maleh, H.; Naddafi, M. A Numerical Solution of Fractional Reaction–Convection–Diffusion for Modeling PEM Fuel Cells Based on a Meshless Approach. *Eng. Anal. Boundary Elem.* **2023**, *155*, 707–716.
- (19) Joghee, P.; Malik, J. N.; Pylypenko, S.; O’Hayre, R. A Review on Direct Methanol Fuel Cells – In the Perspective of Energy and Sustainability. *MRS Energy Sustainable* **2015**, *2* (1), E3.
- (20) Zhao, S.; Yin, H.; Du, L.; Yin, G.; Tang, Z.; Liu, S. Three Dimensional N-Doped Graphene/PtRu Nanoparticle Hybrids as High Performance Anode for Direct Methanol Fuel Cells. *J. Mater. Chem. A* **2014**, *2* (11), 3719–3724.
- (21) Ong, S.; Al-Othman, A.; Tawalbeh, M. Emerging Technologies in Prognostics for Fuel Cells Including Direct Hydrocarbon Fuel Cells. *Energy* **2023**, *277*, No. 127721.
- (22) Eswaraditya Reddy, L.; Gollapudi, D.; Mahnot Jain, G.; Kolluru, S.; Ramesh, G. V. Recent Progress in the Development of Platinum-Based Electrocatalysts for the Oxidation of Ethanol in Fuel Cells. *Mater. Today: Proc.* **2023**, DOI: 10.1016/j.matpr.2023.04.135.
- (23) Xia, C.; Joo, S.-W.; Hojjati-Najafabadi, A.; Xie, H.; Wu, Y.; Mashifana, T.; Vasseghian, Y. Latest Advances in Layered Covalent Organic Frameworks for Water and Wastewater Treatment. *Chemosphere* **2023**, *329*, No. 138580.
- (24) G, A.; Priyadarshini, R.; Titus, A.; Sahoo, S.; Muppala, C.; Ramkumar, G.; Anh Pham, Q.; Rubavathy, S. J.; Rajasimman, M.; Hojjati-Najafabadi, A. Deep Learning for the Encounter of Inorganic Nanomaterial for Efficient Photochemical Hydrogen Production. *Int. J. Hydrogen Energy* **2023**, DOI: 10.1016/j.ijhydene.2023.05.171.
- (25) Nimir, W.; Al-Othman, A.; Tawalbeh, M.; Al Makky, A.; Ali, A.; Karimi-Maleh, H.; Karimi, F.; Karaman, C. Approaches towards the Development of Heteropolyacid-Based High Temperature Membranes for PEM Fuel Cells. *Int. J. Hydrogen Energy* **2023**, *48* (17), 6638–6656.
- (26) Neeshma, M.; Dhanasekaran, P.; Unni, S. M.; Bhat, S. D. Short Side Chain Perfluorosulfonic Acid Composite Membrane with

Covalently Grafted Cup Stacked Carbon Nanofibers for Polymer Electrolyte Fuel Cells. *J. Membr. Sci.* **2023**, *668*, No. 121240.

(27) Bayat, R.; Darabi, R.; Coguplugil, Z. K.; Akin, M.; Bekmezci, M.; Sen, F.; Karimi, F. Synthesis and Applications of Highly Stable Silane Modified Reduced Graphene Oxide Supported Cobalt Based Platinum Nanoparticle for Anodic Part of Direct Methanol Fuel Cells. *Int. J. Hydrogen Energy* **2023**, DOI: 10.1016/j.ijhydene.2023.01.325.

(28) B, M.; Balaji, S. Platinum Studied Synthetic Clay and Nafion Matrix Electrocatalyst for the Oxidation of Methanol in Acid and Alkaline Media For DMFC SSRN *Electron. J.* **2023**, DOI: 10.2139/SSRN.4345485.

(29) Burhan, H.; Arikan, K.; Alma, M. H.; Nas, M. S.; Karimi-Maleh, H.; Sen, F.; Karimi, F.; Vasseghian, Y. Highly Efficient Carbon Hybrid Supported Catalysts Using Nano-Architecture as Anode Catalysts for Direct Methanol Fuel Cells. *Int. J. Hydrogen Energy* **2023**, *48* (17), 6657–6665.

(30) Khan, M. A.; Ramzan, F.; Ali, M.; Zubair, M.; Mehmood, M. Q.; Massoud, Y.; et al. *Nanomater.* **2023**, *13* (4), 780.

(31) Zhao, B.; Fu, J.; Zhou, C.; Yu, L.; Qiu, M.; et al. *Small* **2023**, *19*, No. 2301917.

(32) Young Park, J.; Young Park, J.; Kim, S. A Study on Electrochemical Property of Pt Nanoparticles on Polyethyleneimine-Decorated Graphene. *J. Phys. Chem. C* **2006**, *157*, 497.

(33) Qiu, J. D.; Wang, G. C.; Liang, R. P.; Xia, X. H.; Yu, H. W. Controllable Deposition of Platinum Nanoparticles on Graphene as an Electrocatalyst for Direct Methanol Fuel Cells. *J. Phys. Chem. C* **2011**, *115* (31), 15639–15645.

(34) Saleh, T. A.; Fadillah, G. Recent Trends in the Design of Chemical Sensors Based on Graphene–Metal Oxide Nanocomposites for the Analysis of Toxic Species and Biomolecules. *TrAC, Trends Anal. Chem.* **2019**, *120*, No. 115660. Elsevier B.V. November.

(35) Ramli, Z. A. C.; Kamarudin, S. K. Platinum-Based Catalysts on Various Carbon Supports and Conducting Polymers for Direct Methanol Fuel Cell Applications: A Review. *Nanoscale Res. Lett.* **2018**, *13* (1), 410.

(36) Akin, M.; Bayat, R.; Erduran, V.; Bekmezci, M.; Isik, I.; Şen, F. Carbon-Based Nanomaterials for Alcohol Fuel Cells. *Nanomater. Direct Alcohol Fuel Cells Charact. Des. Electrocatal.* **2021**, 319–336.

(37) Erduran, V.; Bekmezci, M.; Akin, M.; Bayat, R.; Isik, I.; Şen, F. Novel Materials Structures and Compositions for Alcohol Oxidation Reaction. *Nanomater. Direct Alcohol Fuel Cells Charact. Des. Electrocatal.* **2021**, 209–249.

(38) Erduran, V.; Bekmezci, M.; Isik, I.; Sen, F. Different Synthesis Methods of Nanomaterials for Direct Alcohol Fuel Cells. In *Nanomaterials for Direct Alcohol Fuel Cells*; Elsevier, 2021; pp 405–431.

(39) Wang, Y.; Zheng, K.; Ding, J.; Guo, H.; Chen, X.; Zhu, T.; Sun, P.; Liu, Y. Ultrasonic Radiation Enhances Percarbonate Oxidation for Improving Anaerobic Digestion of Waste Activated Sludge. *Chem. Eng. J.* **2023**, *457*, No. 141178.

(40) Liu, T.; Zhang, X.; Liu, M.; Wu, W.; Liu, K.; Liu, Y.; Gu, Y.; Zhang, R. One-Step Room-Temperature Exfoliation of Graphite to 100% Few-Layer Graphene with High Quality and Large Size. *J. Mater. Chem. C* **2018**, *6* (31), 8343–8348.

(41) Coguplugil, Z. K.; Akin, M.; Bayat, R.; Bekmezci, M.; Karimi-Maleh, H.; Javadi, A.; Sen, F. Synthesis and Characterization of Pt/ZnO@SWCNT/Fe<sub>3</sub>O<sub>4</sub> as a Powerful Catalyst for Anodic Part of Direct Methanol Fuel Cell Reaction. *Int. J. Hydrogen Energy* **2023**, *48*, 21285.

(42) Bekmezci, M.; Gules, G. N.; Bayat, R.; Sen, F. Modification of Multi-Walled Carbon Nanotubes with Platinum–Osmium to Develop Stable Catalysts for Direct Methanol Fuel Cells. *Anal. Methods* **2023**, *15* (9), 1223–1229.

(43) Tale, B.; Nemade, K. R.; Tekade, P. V. Graphene Based Nano-Composites for Efficient Energy Conversion and Storage in Solar Cells and Supercapacitors: A Review. *Polym. Technol. Mater.* **2021**, *00*, 1–14.

(44) Daniels, T. M.; Sreearunothai, P.; Phokharatkul, D.; Jomphoak, A.; Pogfay, T.; Nuntawong, N. Flexible, Graphene Protected Ag

Nanoparticles–Polyimide Tape for Use as a Transparent Surface-Enhanced Raman Scattering (SERS) Substrate and Its Application in Pesticide Detection. *Nano-Struct. Nano-Objects* **2023**, *33*, No. 100930.

(45) Almeida, C. V. S.; Huang, H.; Russell, A. E.; Eguiluz, K. I. B.; Salazar-Banda, G. R. Improving the Catalytic Activity of Pt-Rh/C towards Ethanol Oxidation through the Addition of Pb. *Electrochim. Acta* **2022**, *431*, No. 141089.

(46) Razaq, A.; Bibi, F.; Zheng, X.; Papadakis, R.; Jafri, S. H. M.; Li, H. Review on Graphene-, Graphene Oxide-, Reduced Graphene Oxide-Based Flexible Composites: From Fabrication to Applications. *Materials* **2022**, *15* (3), 1012.

(47) Gayathri, S.; Jayabal, P.; Kottaisamy, M.; Ramakrishnan, V. Synthesis of Few Layer Graphene by Direct Exfoliation of Graphite and a Raman Spectroscopic Study. *AIP Adv.* **2014**, *4* (2), No. 027116.

(48) Park, M. H.; Kim, T. H.; Yang, C. W. Thickness Contrast of Few-Layered Graphene in SEM. *Surf. Interface Anal.* **2012**, *44* (11–12), 1538–1541.

(49) Childres, I.; Jauregui, L. A.; Park, W.; Cao, H.; Chen, Y. P. Raman Spectroscopy of Graphene and Related Materials. In *New Developments in Photon and Materials Research*; 2013; Vol. 1, pp 1–20.

(50) Ni, Z.; Wang, Y.; Yu, T.; Shen, Z. Raman Spectroscopy and Imaging of Graphene. *Nano Res.* **2008**, *1* (4), 273–291.

(51) Venezuela, P.; Lazzeri, M.; Mauri, F. Theory of Double-Resonant Raman Spectra in Graphene: Intensity and Line Shape of Defect-Induced and Two-Phonon Bands. *Phys. Rev. B* **2011**, *84* (3), No. 035433.

(52) Wang, B.; Chen, B.; Sun, Y.; Xiao, H.; Xu, X.; Fu, M.; Wu, J.; Chen, L.; Ye, D. Effects of Dielectric Barrier Discharge Plasma on the Catalytic Activity of Pt/CeO<sub>2</sub> Catalysts. *Appl. Catal., B* **2018**, *238*, 328–338.

(53) Kumar, V.; Kumar, A.; Lee, D.-J.; Park, S.-S. Estimation of Number of Graphene Layers Using Different Methods: A Focused Review. *Materials* **2021**, *14* (16), 4590.

(54) Liu, Y.; Goolaup, S.; Murapaka, C.; Lew, W. S.; Wong, S. K. Effect of Magnetic Field on the Electronic Transport in Trilayer Graphene. *ACS Nano* **2010**, *4* (12), 7087–7092.

(55) Wu, Y.; Yuan, Y.; Shuang, W.; Wang, L.; Yang, L.; Bai, Z.; Lu, J. Reducing Carbonaceous Salts for Facile Fabrication of Monolayer Graphene. *Small Methods* **2023**, *7* (3), No. 2201596.

(56) Jinxi, W.; Aimin, W.; Ghasemi, A. K.; Lashkenari, M. S.; Pashai, E.; Karaman, C.; Niculina, D. E.; Karimi-Maleh, H. Tailoring of ZnFe<sub>2</sub>O<sub>4</sub>-ZrO<sub>2</sub>-Based Nanoarchitectures Catalyst for Supercapacitor Electrode Material and Methanol Oxidation Reaction. *Fuel* **2023**, *334* (P1), No. 126685.

(57) Li, F.; Chang, X.; Wang, S.; Guo, Y.; Li, H.; Wu, K. Excellent Electrocatalytic Performance toward Methanol Oxidation of Hierarchical Porous NiCu Obtained by Electrochemical Dealloying. *J. Alloys Compd.* **2023**, *934*, No. 167811.

(58) Haskul, M.; Ülgen, A. T.; Döner, A. Fabrication and Characterization of Ni Modified TiO<sub>2</sub> Electrode as Anode Material for Direct Methanol Fuel Cell. *Int. J. Hydrogen Energy* **2020**, *45* (7), 4860–4874.

(59) Li, M.; Shi, J.; Guo, X.; Ying, Y.; Wu, Y.; Wen, Y.; Yang, H. PdMo Supported by Graphene for Synergistic Boosting Electrochemical Catalysis of Methanol Oxidation. *J. Electroanal. Chem.* **2023**, *928*, No. 117038.

(60) Chandra Sekhar, Y.; Raghavendra, P.; Sri Chandana, P.; Maiyalagan, T.; Subramanyam Sarma, L. Graphene Supported Pd–Cu Bimetallic Nanoparticles as Efficient Catalyst for Electrooxidation of Methanol in Alkaline Media. *J. Phys. Chem. Solids* **2023**, *174*, No. 111133.

(61) Pham, H. Q.; Huynh, T. T. Facile Room-Temperature Fabrication of a Silver-Platinum Nanocoral Catalyst towards Hydrogen Evolution and Methanol Electro-Oxidation. *Mater. Adv.* **2022**, *3* (3), 1609–1616.

(62) Zhang, Q.; Xia, T.; Huang, H.; Liu, J.; Zhu, M.; Yu, H.; Xu, W.; Huo, Y.; He, C.; Shen, S.; Lu, C.; Wang, R.; Wang, S. Autocatalytic Reduction-Assisted Synthesis of Segmented Porous PtTe Nanochains



for Enhancing Methanol Oxidation Reaction. *Nano Res. Energy* **2023**, *2*, No. e9120041.

(63) Ren, Y.; Zang, Z.; Lv, C.; Li, B.; Li, L.; Yang, X.; Lu, Z.; Yu, X.; Zhang, X. Structurally-Supported PtCuCo Nanoframes as Efficient Bifunctional Catalysts for Oxygen Reduction and Methanol Oxidation Reactions. *J. Colloid Interface Sci.* **2023**, *640*, 801–808.

(64) Martinez-Mora, O.; Leon-Fernandez, L. F.; Velimirovic, M.; Vanhaecke, F.; Tirez, K.; Fransaeer, J.; Dominguez-Benetton, X. Platinum Nanoclusters Made by Gas-Diffusion Electrocrystallization (GDEx) as Electrocatalysts for Methanol Oxidation. *Mater. Adv.* **2023**, DOI: [10.1039/D3MA00209H](https://doi.org/10.1039/D3MA00209H).

(65) Bayat, R.; Burhan, H.; Bekmezci, M.; Isgin, E. S.; Akin, M.; Sen, F. Synthesis and Characterization of Lignin-Based Carbon Nanofiber Supported Platinum–Ruthenium Nanoparticles Obtained from Wood Sawdust and Applications in Alcohol Fuel Cells. *Int. J. Hydrogen Energy* **2023**, *48* (55), 21128–21138.

(66) Karimi, F.; Akin, M.; Bayat, R.; Bekmezci, M.; Darabi, R.; Aghapour, E.; Sen, F. Application of Quasihexagonal Pt@PdS<sub>2</sub>-MWCNT Catalyst with High Electrochemical Performance for Electro-Oxidation of Methanol, 2-Propanol, and Glycerol Alcohols For Fuel Cells. *Mol. Catal.* **2023**, *536*, No. 112874.